

MEASURING THE MORPHOLOGY AND DYNAMICS OF THE SNAKE RIVER BY REMOTE SENSING

CARL J. LEGLEITER ✦ UNIVERSITY OF WYOMING ✦ LARAMIE

✦ ABSTRACT

The Snake River is a central component of Grand Teton National Park, and this dynamic fluvial system plays a key role in shaping the landscape and creating diverse aquatic and terrestrial habitat. The river's complexity and propensity for change make effective characterization of this resource difficult, however, and conventional, ground-based methods are simply inadequate. Remote sensing provides an appealing alternative approach that could facilitate resource management while providing novel insight on the factors controlling channel form and behavior. In this study, we evaluate the potential to measure the morphology and dynamics of a large, complex river system such as the Snake using optical image data. Initially, we made use of existing, publicly available images and basic digital aerial photography acquired in August 2010. Analysis to date has focused on estimating flow depths from these data, and preliminary results indicate that remote bathymetric mapping is feasible but not highly accurate, with important constraints related to the limited radiometric resolution of these data sets. Additional, more sophisticated hyperspectral data are scheduled for collection in 2011, along with further field work.

✦ INTRODUCTION

A defining feature of the Teton landscape, the Snake River (Figure 1) plays an important role in the geomorphology and ecology of Jackson Hole while providing visitors to Grand Teton National Park with an abundance of recreational opportunities. This dynamic fluvial system collects water and sediment from a large, mountainous drainage basin

and conveys these materials across the valley floor via various mechanisms of flow and sediment



Figure 1.

transport. These processes interact to produce coherent patterns of sediment transfer and storage that are manifested as distinctive landforms - channels, bars, floodplains, and terraces. These geomorphic surfaces are colonized by vegetative communities but eventually reclaimed as the river shifts laterally, incises new channels, or reoccupies former flow paths. This perpetual reworking of the riparian zone creates a patchy mosaic of habitat

conditions that supports a diversity of terrestrial and aquatic organisms, including such iconic species as bald eagles, beaver, native trout, and moose. The potential to view such wildlife, along with the unique scenery in part created by the Snake, makes this fluvial environment a source of considerable enjoyment by the public, for whom the river and surrounding National Park have been protected and preserved.

Managing these natural resources is the task of the National Park Service, but efforts to achieve this objective are complicated by the same dynamism and complexity that make the Snake River such a vibrant element of the landscape. Basic information on the river's form and behavior are needed for resource assessment and monitoring purposes, but the logistical constraints associated with conventional field methods make obtaining even sparse data difficult. Measuring channel and floodplain topography, flow conditions, and streambed characteristics over long reaches is simply not feasible in such a heterogeneous riverine environment. Moreover, the channel changes that occur during each spring's snowmelt imply that maintaining an accurate, current database would require annual surveys. Information of this kind would facilitate various ongoing ecological and geomorphic investigations while enabling the Park Service to more readily achieve certain management objectives. For example, studies of native cutthroat trout would benefit from a more detailed knowledge of the physical habitat conditions (e.g., depth, velocity, and bed material grain size) preferred by these species during different life stages. Similarly, research on the effects of flow regulation on floodplain inundation, bed mobility, and general channel stability, along with related efforts to develop reach-scale sediment budgets, would benefit from more extensive, higher resolution topographic data. For resource management, current information on channel depths, the distribution of bars, and the location of obstructions (e.g., accumulations of large woody debris) would allow navigability by rafts to be assessed more easily and could help recreational boaters to avoid potentially hazardous situations. For many reasons, then, an enhanced capacity to characterize the morphology and dynamics of the Snake River would be of great value.

Remote sensing techniques could provide such a capacity by enabling more efficient measurement of several key river attributes. A quantitative, remote sensing-based approach would have several distinct advantages in this context: 1) a synoptic perspective that allows long segments of

broad riparian zones to be mapped in a matter of hours rather than weeks; 2) continuous, high-resolution data that capture the spatial variability of the riverine environment far more effectively than traditional methods based on isolated cross-sections; and 3) more frequent coverage that could not only facilitate monitoring but also lead to an improved understanding of the fluvial processes that drive channel change and thus create, modify, and maintain diverse terrestrial and aquatic habitats.

Research on the application of remote sensing to rivers has grown considerably over the past decade (Marcus and Fonstad, 2010), and recent studies have demonstrated the feasibility of mapping flow depth from optical image data (Legleiter et al., 2004, 2009). Similarly, the development of Light Detection and Ranging (LiDAR) technology (Slatton et al. 2007) allows the topography of exposed bars and floodplains to be measured with a high degree of accuracy; LiDAR data can also be used to estimate water surface slopes (Hofle et al., 2009), identify off-channel habitats, and derive information on riparian vegetation. Integrated, spatially explicit analysis of remotely sensed data can thus enable scientists and managers to efficiently characterize complex river systems like the Snake.

Research hypothesis and specific aims

The primary goal of our ongoing research is to use remote sensing methods to gain leverage for addressing an important, challenging problem of keen scientific interest and direct relevance to current management needs: characterizing the morphology and dynamics of the Snake River. This effort will facilitate the Park Service's efforts to protect this resource, contribute to several ongoing studies, and yield insight on the factors controlling channel form and behavior. We have a more general research interest in remote sensing of rivers, but the Snake River in Grand Teton National Park is one of the primary field sites we are using to develop and test new methods. Importantly, this dynamic fluvial environment provides an opportunity to critically evaluate the feasibility of mapping a large, complex river system from various types of image data. This project is also consistent with the overarching motivation for our research program: to achieve a quantitative understanding of the manner in which flow and sediment transport processes interact with channel form to direct a river's morphologic evolution. To support our pursuit of these broader objectives, the pilot study conducted in 2010 addressed the following specific aims:

1) Identify, compile, and organize various remotely sensed data sets potentially useful for characterizing the Snake River in Grand Teton National Park.

2) Develop and apply various image processing techniques and mapping algorithms for deriving river information from these data; attributes of interest include flow depth, water surface slope, and channel and floodplain topography.

3) Obtain field measurements of bed topography and flow conditions to assess the accuracy of image-derived estimates.

4) Explore ways in which remotely sensed river information can contribute to various scientific investigations and river management objectives and establish collaborations with researchers and agency personnel.

5) Determine future research needs and plan collection of additional remotely sensed and field data that will provide a more thorough, better-validated characterization of the Snake River.

◆ STUDY AREA

This effort to characterize channel morphodynamics via remote sensing focuses on the Snake River corridor within Grand Teton National Park. This dynamic fluvial system represents, in many respects, an ideal location for this study because the river encompasses a range of channel morphologies, valley floor environments, and disturbance regimes that will not only present a challenging test of remote sensing methods but also allow us to examine various controls on channel form and behavior. For example, the Snake includes both meandering and braided segments that are influenced by differences in slope, variations in sediment supply, diverse riparian vegetation, and a strong tectonic signal. Field measurements and remotely sensed data along the Snake thus allow us to draw comparisons among a variety of stream reaches in terms of both their suitability for remote mapping and geomorphic controls on their form and behavior. In addition, the Snake is an attractive site for study because the river features: 1) typically clear water conditions conducive to remote sensing of flow depths; 2) a pair of stream gages that provide a continuous record of river discharge; 3) relatively little direct human impact, apart from flow regulation by Jackson Lake Dam; and 4) a well-documented record of channel change based on historical aerial photography

(Schmidt and Nelson, 2007). Many reaches of the Snake River experience significant channel changes each year during high-magnitude flow events associated with snowmelt runoff, and both existing and planned remotely sensed data sets provide an effective means of characterizing these dynamics.

The initial pilot study we conducted in 2010 involved field data collection at a number of sites along the riparian corridor, identifying locations that span a range of depths, channel geometries, and riparian vegetation communities. Our efforts were focused on the segment between Pacific Creek and Moose, with the most intensive data collection performed at the meander bend located at 537500 m E, 4851200 m N (UTM Zone 12N). In addition, we performed a longitudinal survey of the Snake River using a cataraft outfitted with equipment for measuring flow depths and velocities.

◆ METHODS

For the preliminary investigation completed in 2010, our general strategy was to: 1) identify and obtain existing remotely sensed data sets potentially useful for characterizing the Snake River; 2) acquire additional multispectral image data from the river corridor; 3) organize these data within a GIS; 4) develop image processing techniques for deriving river information from various kinds of remotely sensed data; and 5) assess the reliability of this information using field measurements. The latter, ground-based observations also provide a basis for planning future remote sensing campaigns, with a series of flights scheduled to occur in August 2011. This project thus involved a combination of geospatial data analysis and field work; these two components are described in the following sections.

Remotely sensed data and image processing

In the initial stage of this ongoing study, our efforts focused on existing remotely sensed data sets and basic digital aerial photography acquired in August 2010. We have recently obtained external funding to support the acquisition of more sophisticated hyperspectral and LiDAR data that will enhance our capacity to measure the morphology and dynamics of the Snake River. Ultimately, the principal channel attributes we intend to map via remote sensing are flow depth, channel bed topography, and water surface slope. Several data sets potentially useful for these purposes were identified, obtained, and compiled in a GIS.

First, digital aerial photography of Grand Teton National Park was acquired under low-flow conditions on August 2, 2009, through the National Agricultural Imagery Program (NAIP). These images comprise four-band data, including a near-infrared (NIR) wavelength, with a spatial resolution (i.e., pixel size) of 1 m, a level of detail sufficient to detect all but the smallest channel features. NAIP data are publicly available over the internet in the form of county-level mosaics, but these files are compressed and we found that these images did not provide the radiometric resolution required to distinguish subtle variations in brightness associated with differences in flow depth. Instead, we obtained the original, uncompressed digital orthophoto quarter-quadrangles (DOQQ's) in a GeoTIFF format from the Wyoming Geographic Information Science Center. A similar NAIP data set was acquired in 2006 and will be used to characterize recent channel changes along the Snake River, but efforts to date have focused on depth mapping from the 2009 data.

To complement these existing NAIP data sets and extend the image time series documenting channel change along the Snake River, we acquired additional digital aerial photography of our study area on August 11, 2010, under similar, low-flow conditions. These data were collected through the Upper Midwest Aerospace Consortium's Aerocam program and consisted of a series of 506 color-infrared images extending from Jackson Lake dam downstream to the Park boundary at Moose. The Aerocam data were delivered as raw TIFF files lacking spatial information and thus had to be georeferenced. We used the ENVI image processing software package to identify common ground control points on the 2009 NAIP DOQQ's and the original Aerocam images, transform the Aerocam data to the UTM coordinate system, and produce a mosaic with a consistent pixel size of 0.5 m. This mosaic consisted of 39 image tiles, with an average georeferencing root mean square error and the average root mean square error (RMSE) of 0.95 m, based on 30-50 control points for each image. In addition to providing a further increment to our time series, the Aerocam data provided an opportunity to collect field data at the same time the images were acquired, which allowed us to directly calibrate image-derived depth estimates and assess their accuracy. This analysis gave us greater confidence in applying similar techniques to older images for which simultaneous field data were not available.

We have recently obtained another valuable data set originally collected in October 2007: LiDAR coverage of the Snake River corridor below Jackson

Lake (Figure 2). In general, LiDAR has become the preferred method for high-resolution, precise measurement of Earth's topography, capable of providing accurate elevation data at densities on the order of 1-4 points/m² (Slatton et al., 2007). The Snake River data set was acquired by a private contractor (Aero-Metric, Inc.), with a reported point spacing of 0.615 m and horizontal and vertical accuracies of 0.18 m and 0.089 m, respectively. Data products include filtered, bare Earth LiDAR point clouds, a digital terrain model, and first return intensity images. In the context of this project, the LiDAR coverage should prove useful for mapping bar surfaces, floodplains, and abandoned channels and their distribution and connectivity along the valley floor (Jones et al., 2007). Moreover, Hofle et al. (2009) have shown that water surface slope can be measured accurately via LiDAR; this important channel attribute influences flow hydraulics and thus patterns of sediment transport and morphologic change. Having only received this data set within the past couple of weeks, our analysis of the LiDAR data is at a very early stage. Ultimately our main objectives are to use the LiDAR terrain model to characterize the topography of bars and floodplains along the Snake River corridor and to estimate water surface slopes from the filtered point clouds. By comparing the 2007 coverage to LiDAR data collected in 2011, we will also be able to measure the vertical dimension of channel change and thus estimate volumes of erosion and deposition.

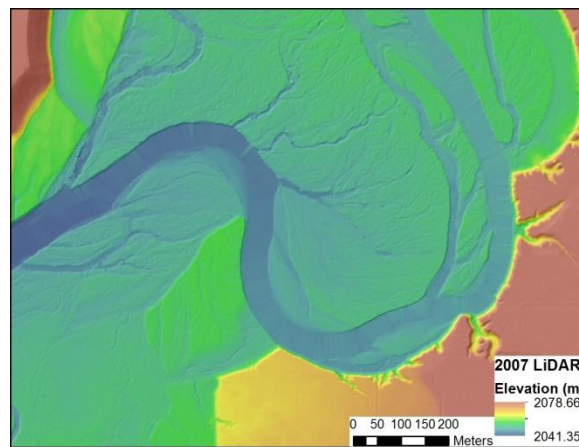


Figure 2. Example of 2007 LiDAR topographic data from the Snake River, with a digital terrain model displayed over a hill-shade image.

Though useful for exposed, terrestrial surfaces, LiDAR fails to provide topographic information from submerged areas due to strong absorption of near-infrared laser pulses by water. An alternative approach is thus needed to characterize

the wetted channel proper. Our previous research has demonstrated that, under appropriate conditions (i.e., relatively shallow, clear water), water depth can be estimated from passive optical image data. More specifically, because the rate at which light is attenuated by the water column varies as a function of wavelength, as depth increases the amount of reflected solar energy recorded in a spectral band experiencing stronger attenuation decreases more rapidly than does the amount of energy measured in a band for which attenuation is weaker. Calculating the logarithm of the ratio of the pixel values for two spectral bands thus yields an image-derived quantity that is linearly related to water depth; calibration is achieved by regressing values of this quantity against depths measured in the field (Legleiter et al., 2009). This approach can be applied directly to the 2010 Aerocam images because these data were acquired in late summer, when concentrations of suspended sediment were minimal, water clarity was high, and field data were collected within a few days of the flight. This ratio-based method was also applied to the 2009 NAIP images, which were also collected under low-flow, clear-water conditions. No field data were available from this time period, however, so, for this preliminary study, the depths measured in 2010 were assumed representative of 2009 as well, except in areas of obvious channel change. We used this simple depth retrieval algorithm to develop bathymetric maps that depict pools, riffles, and shallow submerged bars for both time periods.

To produce a complete topographic representation of the riverine environment, LiDAR topography and spectrally-based bathymetry can be combined into a single digital terrain model. The LiDAR provides elevation measurements for exposed areas, and bed elevations within the channel can be determined by subtracting spectrally-based depth estimates from water surface elevations recorded for LiDAR points along the edge of the water. Some adjustment might be necessary to account for differences in flow level if the LiDAR and optical data were not acquired simultaneously, but this offset can be determined from gage heights recorded at Jackson Lake and Moose on each date. Because we only recently received the 2007 LiDAR coverage and this data set obviously represents a different time period, we have not performed this analysis but should have an opportunity to do so using the LiDAR and optical data scheduled for collection in 2011.

Field data collection

In addition to this geospatial data analysis, our study also involved extensive field work, both to

validate remotely sensed river information and to support our overall geomorphic research interests. A key component of this field effort was a survey of channel and floodplain topography. These data were collected using a high-precision (sub-centimeter) real-time kinematic GPS receiver that was attached to a survey rod for measuring terrestrial surface elevations (Figure 3). Survey points were arranged along cross-sections and selected so as to emphasize important breaks in slope and key morphologic features such as the top and base of stream banks. Data were collected for the full width of the riparian zone but were concentrated within the shallow portion of the active channel. For areas that were too deep to wade safely, the GPS receiver was mounted on our cataraft and configured to record water surface elevations while communicating with an echo sounder that measures flow depths; subtracting the depth from the water surface elevation yielded measurements of the bed elevation. These data, along with direct depth measurements made by wading in shallow areas, allowed us to relate flow depths to spectrally-based quantities derived from the Aerocam and NAIP images. These field surveys also provided a means of assessing the accuracy of topographic data obtained via remote sensing.

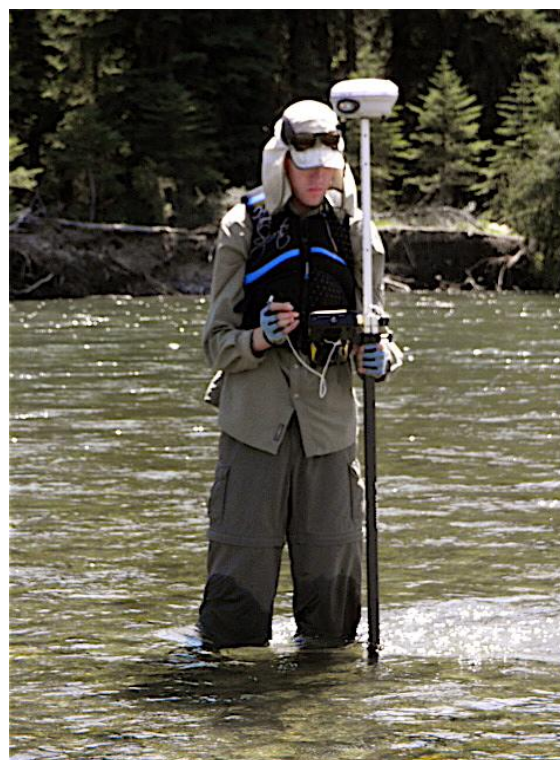


Figure 3. Field data collection along the Snake River. Bed elevations and flow depths were recorded with a high-precision real-time kinematic GPS receiver, via wading in shallow areas or from a cataraft equipped with an echo sounder in deeper portions of the channel.

In an effort to better characterize and understand the fluvial processes driving the channel changes observed in our image time series, we measured flow conditions within the Snake River. Our cataraft was outfitted with an acoustic Doppler current profiler (ADCP) that measured flow velocities in a series of cells distributed vertically throughout the water column. This instrument recorded streamwise, cross-stream, and vertical velocity components at a frequency of once per second and thus provided a very detailed characterization of the flow field. We used the ADCP to measure river discharge by integrating the product of depth and velocity as we moved across the channel. Our discharge measurement protocol required that the boat remain stationary at the beginning and end of each cross-section, and maintaining a fixed position with oars alone proved difficult, as did traversing the channel in a straight line across strong currents. For 2011, we have requested permission to use a small electric trolling motor to facilitate our field measurements. In addition to the cross-sections, which were distributed throughout the study area but concentrated in a few key reaches, we also recorded flow depths and velocities along a series of profiles oriented down the river. The data we acquired with the ADCP will support future work focused on the interactions between flow processes, bed material transport, and the evolution of channel form.

✦ PRELIMINARY RESULTS

2010 was the first year of this study, and we enjoyed a highly productive field campaign in early August, and digital aerial photography of the Snake River corridor were successfully acquired on August 11. To date, our analysis has focused on retrieving water depth from these images, processing topographic surveys, and summarizing the hydraulic information collected with the ADCP. The following sections report some of our initial findings and discuss our plans for further work along the Snake.

Mapping flow depth from remotely sensed data

In addition to their more traditional role as a means of recording changes in channel planform, remotely sensed data can be used to quantify spatial variations in flow depth, adding a third dimension to the description of river morphology and dynamics. In this study, we used the band-ratio based algorithm described above to estimate water depths from both the Aerocam images acquired in 2010 and NAIP data

from 2009. Various band combinations were considered, but the green and red wavelengths appeared the most promising, as suggested by an earlier study based on radiative transfer modeling (Legleiter et al., 2004). To isolate the in-stream portion of each image, we created a mask by digitizing the wetted channel, excluding any exposed bars or shadows that obscured the stream. We then extracted pixel values from the locations of the ground-based depth measurements obtained via wading or with the cataraft-mounted echo sounder. An image-derived quantity X , found in previous studies to be linearly related to flow depth (Legleiter et al., 2009), was calculated as $X = \ln(G/R)$, where G and R denote the pixel values in the green and red bands, respectively. Calibration involved correlating X values with the ground-based measurements of depth d via linear regression. The data subjected to regression analysis consisted of all of the wading-based depth measurements, which were relatively few in number and concentrated in shallow areas less than 1.1 m deep, and a random sample of depths recorded by the echo sounder. This instrument provided continuous measurements and thus a much larger number of data ($n = 33,865$ over the course of our surveys) from throughout the channel, including areas up to 3.57 m deep, but could not resolve depths less than 0.3 m and was generally less reliable in shallower water. To provide a more even, representative sampling across the full range of depths, we combined the wading data with an equivalent number of randomly sampled echo sounder depths greater than 0.9 m. The equation resulting from this regression analysis was then applied throughout the in-stream portion of the image to produce a bathymetric map. Accuracy was assessed by comparing image-derived estimates to surveyed depths via plots of cross-sections and longitudinal profiles that encompassed a range of channel morphologies.

The following figures summarize the results of this analysis for a typical Aerocam image (#427) from the lower portion of our study area. The green and red bands were used to calculate X values, which were then calibrated to measured flow depths d via linear regression with an R^2 of 0.55, indicating a moderately strong linear relationship between the image-derived quantity and depth (Figure 4). The standard error of 0.33 m was 38% of the mean (0.85 m) of the 64 depths used for calibration, however, and the scatter plot below indicates that the X vs. d relation was weaker for greater depths > 1.5 m.

This regression equation was applied to the in-stream portion of the image to produce the

bathymetric map depicted below. Although the geo-referenced Aerocam images had a nominal spatial resolution of 0.5 m, the data were quite noisy, and this pixel-to-pixel variability was accentuated by the ratio calculation and logarithmic transformation. To diminish this grainy texture, we applied a Weiner spatial filter to both the green and red bands prior to computing X values and then again to the resulting band ratio image. This procedure improved the image quality to an extent, but the bathymetric map remained rather pixilated. Note that some of this noise could be the inevitable consequence of sun glint from the water surface. In general, however, the image-derived depth map effectively captured the gross morphology of the channel, with, for example, greater depths along the outer bank on the lower left side of the map below, and shallower flow over the point bar on the inside of the bend.

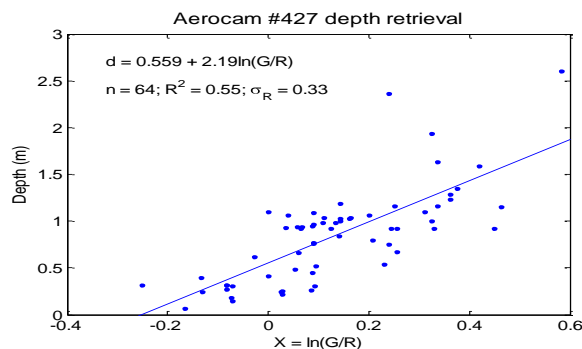


Figure 4. Regression analysis used to calibrate the image-derived quantity X to field-based depth measurements of for an Aerocam image of the Snake River near Moose.

As an indication of the accuracy of the remotely sensed river information, image-derived depth estimates were compared to a cross-section from the side-channel (labeled XS #1 on the map) and a longitudinal profile (#212) through the meander bend at the lower end of the reach (Figure 5). The cross-section below indicates good overall agreement between the image-derived depth estimates and the field survey, with depth increasing from the left (facing downstream) bank toward the base of the terrace on the right side of the channel, although depth tended to be over-estimated in shallower water. For the longitudinal profile shown above, the noise associated with the image-derived depth estimates is evident as a pronounced spiky pattern superimposed on the overall trend of the morphology (Figure 6). The remotely sensed bathymetry closely matches the echo sounder measurements for the first 100 m of the profile but then underestimates the depth through the apex of the bend, where measured depths exceeded 2.5 m but the image-derived estimates remained on the order of 1.3 m. Where the flow shoaled at the

lower end of this pool, agreement improved. The observed under-prediction of depth in deeper water was expected and resulted from the low radiometric resolution of the Aerocam images. These data were recorded in 8-bit digital form, with only 256 possible values spanning the full range of brightness from dry gravel bars to the deepest pools. Each of these digital numbers thus represented a large change in radiance, and the relatively small reductions in radiance that occurred as the flow became deeper were thus beyond the detection limit of this basic imaging system. This saturation of the radiance signal in deeper water is an important limitation of spectrally-based bathymetric mapping that implies that the full depth of pools might not be resolved.

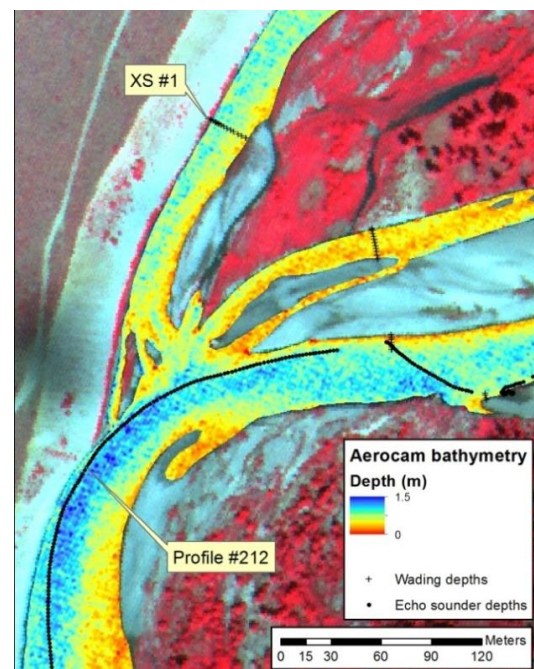


Figure 5. Bathymetric map derived from an Aerocam image. Also indicated are the locations of the cross-section and longitudinal profile shown in the following figures. Flow is to the south, from top to bottom on the image.

To evaluate depth retrieval performance for both the 2010 Aerocam and 2009 NAIP images, we considered another site located farther upstream, closer to Pacific Creek. The analysis for this reach, corresponding to Aerocam image #612, proceeded in a manner similar to that described above in the context of image #427: an in-stream mask was digitized, pixel values were extracted from depth measurement locations, X values were calculated as $\ln(G/R)$, and regression performed using all wading measurements and a random sample of echo sounder depths greater than 0.9 m. Results of the X vs. d calibration for the 2009 NAIP image are summarized in Figure 7.

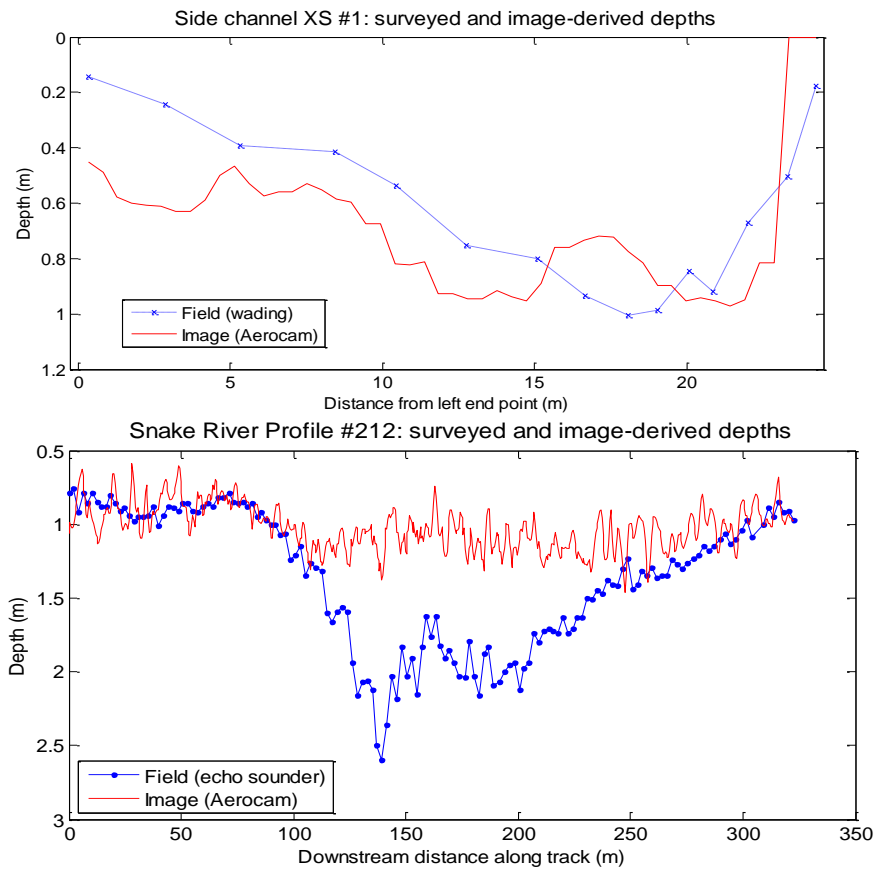


Figure 6. Comparison of field measurements and image-derived depth estimates for the cross-section (top) and longitudinal profile (bottom) indicated in Figure 5.

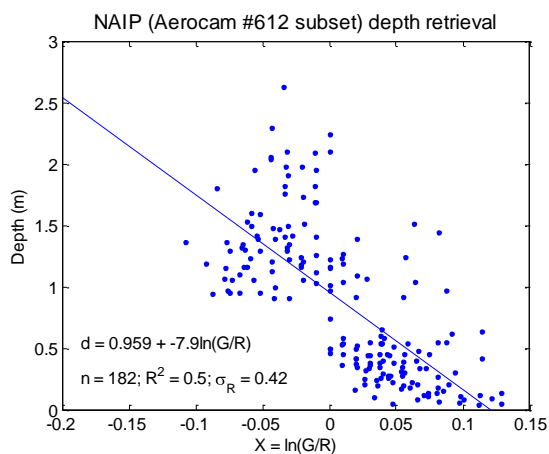


Figure 7. Regression analysis used to calibrate the image-derived quantity X to field-based depth measurements of for an NAIP image subset downstream from Pacific Creek.

The correlation between X and d was moderately strong ($R^2 = 0.50$) and slightly greater than that for the Aerocam image of this site ($R^2 = 0.45$). The image-derived quantity was inversely

related to depth, however. This result was unexpected because red light is attenuated more rapidly by the water column than is green light, implying a direct relation between X and d when the green band is used as the band ratio numerator (Legleiter et al., 2009). We attribute the inverse relationship observed here to modification of the original radiance measurements that occurred during post-processing of the NAIP images. Because this program is intended to support agricultural monitoring, the raw data are subjected to a color balancing procedure to maintain a constant image tone between individual scenes and over time. In this case, we infer that the green band was adjusted downward and the red band adjusted upward, which had the effect of reversing the relationship between depth and digital numbers for these two bands. Similarly, the green and red bands might have had different gains and offsets for converting at-sensor radiance to digital numbers. In any case, these results clearly illustrate an important point: depth retrieval from image data that have not been radiometrically calibrated is purely empirical and hence scene-specific. Establishing more robust, general relationships between image-derived quantities and

flow depths will require image data calibrated to physical units of radiance, rather than digital numbers, and no manipulation of the original measurements during subsequent image processing.

Nevertheless, given the large sample of field data available for calibration, the bathymetric map derived from the 2009 NAIP image was coherent and hydraulically reasonable. Shallow depths were predicted from the image along the margins of the channel and over the point bars present in this sinuous reach. Greater depths were correctly identified where the channel talweg shifted from the right bank opposite the large bar at the bottom of the image to the left bank along the outside of the bend and then back to the right bank where the channel curved to the west at the lower end of the reach. The bathymetric map derived from the NAIP data was also noticeably less noisy than that produced from the corresponding Aerocam image. These results imply that depth retrieval from existing, publicly available image data might be feasible.

A comparison of predicted vs. observed depths, however, indicates that such image-derived estimates might not be very reliable and will be subject to some key limitations. The figure below compares depths measured in the field to estimates from the Aerocam and NAIP images for an asymmetrical cross-section past the apex of the large meander bend in Figure 8 and a longitudinal profile through the next bend downstream, where the river curves to the left. Both of these plots show the spikier texture of the bathymetry derived from the Aerocam images and the relatively smoothly varying depths inferred from the NAIP data. For the cross-section, both images yielded depths similar to those measured in the field on the shallower right side of the transect but failed to resolve the full depth of the pool located near the outer (left) bank. Again, this result can be attributed to saturation of the radiance signal in deeper water, along with the limited radiometric resolution of these 8-bit data sets. For the longitudinal profile, the NAIP bathymetry closely tracks the echo sounder depths for the first 285 m. The divergence that occurs at that point could reflect actual channel change as the point bar on the left bank grew and extended laterally into the channel, resulting in shallower depths in 2010 than in 2009, when the NAIP data were acquired. Depths within the pool along the outer (right) bank were more accurately estimated from the NAIP image than from the Aerocam scene, but the gaps in the profile extracted from the NAIP bathymetry reflect the

presence of shadows cast by tall pines on the bank (Figure 8,9). This observation highlights another fundamental limitation for remote sensing of rivers: an unobstructed view of the stream is required, limiting the applicability of this approach in smaller, forested channels and constraining the time of day and season of the year when useful images can be acquired.

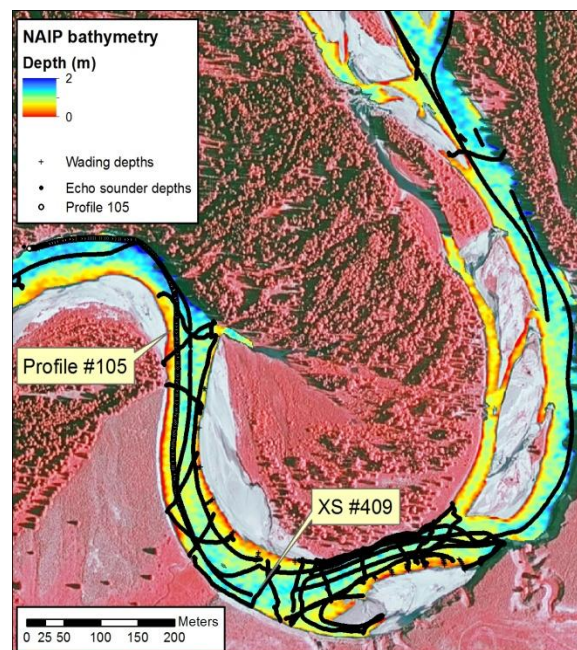


Figure 8. Bathymetric map derived from a 2009 NAIP image. Also indicated are the locations of the cross-section and longitudinal profile shown in the following figure. Flow is to the south, from the top of the image to the bottom and then exiting on the left side of the scene.

In general, our results suggest that spectrally-based bathymetric mapping from basic optical image data is feasible, but not highly accurate. This approach can thus provide an informative, qualitative impression of the gross morphology of a channel, but obtaining precise measurements of bed elevation to serve as topographic input data for hydraulic modeling or for quantifying erosion and deposition are likely to require more sophisticated hyperspectral image data with greater radiometric resolution. We intend to acquire such data in 2011 and will evaluate the extent to which reliable river information needed to support more demanding applications can be obtained via remote sensing. Although the potential for remote mapping of fluvial systems is clearly significant, the inherent limitations of this approach must be borne in mind as well.

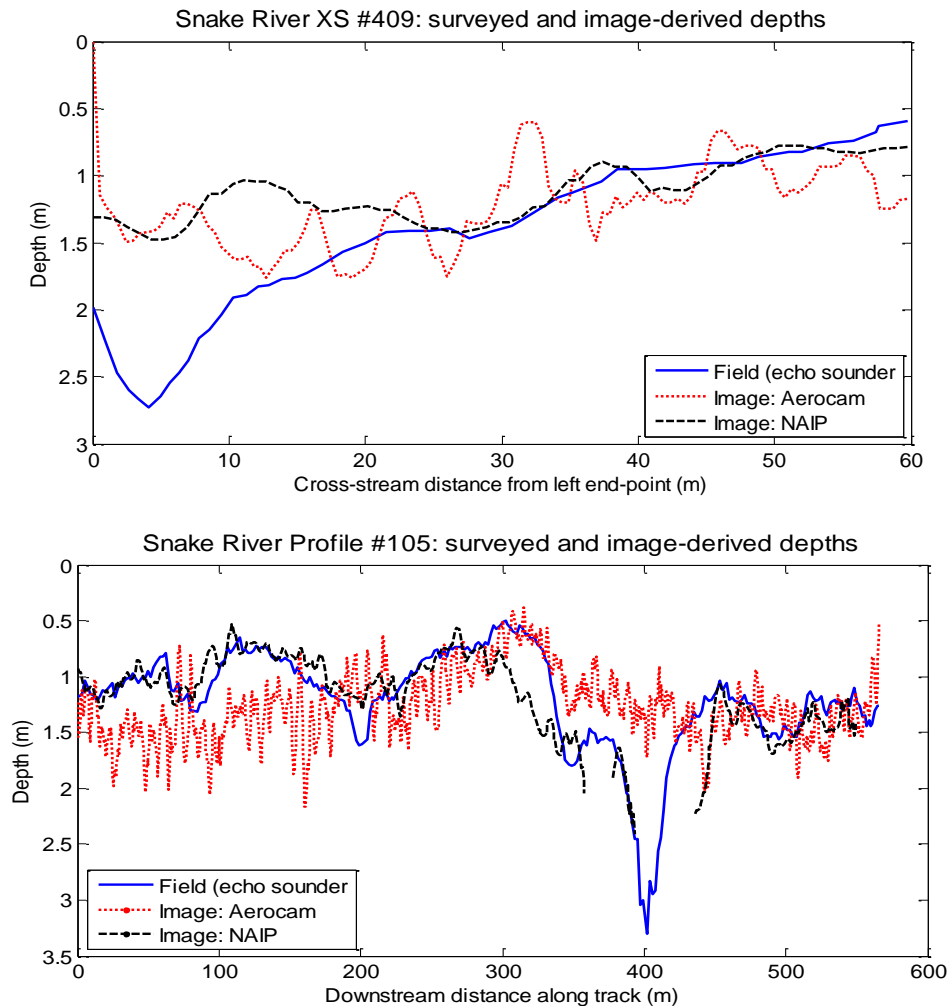


Figure 9. Comparison of field measurements and depth estimates derived from the Aerocam and NAIP images for the cross-section and long profile indicated in Figure 8.

Field measurements of river morphology and hydraulics

In addition to field surveys of channel and floodplain topography, we also used an acoustic Doppler current profiler (ADCP) deployed via cataraft to measure flow velocities on a series of cross-sections and longitudinal profiles distributed throughout our study area along the Snake River (Figure 10). This new instrument provided a wealth of hydraulic information, including observations of three-dimensional velocity components in a set of vertical cells distributed throughout the water column, recorded at a frequency of once per second as the cataraft navigated along and across the river. These data thus yield a detailed depiction of the flow patterns that determine the magnitude and orientation of fluid forces that in turn mobilize and transport sediment and thus dictate the trajectory of channel

change. Though not directly relevant to remote sensing, the ADCP data will help us to understand the geomorphic processes responsible for the river dynamics observed in our image time series.

We have made significant progress in our analysis of the ADCP data sets collected in 2010, but only a couple of examples are presented here to illustrate the kind of information we have obtained. Much of our effort to date has gone toward the development of computer code to ingest, organize, and summarize the massive volume of data acquired during a single ADCP transect. Our MATLAB functions determine the orientation of a cross-section, project the data into a channel-centered coordinate system, resolve the velocity vector into downstream and cross-stream components, compute depth-averaged velocity magnitudes, produce graphical

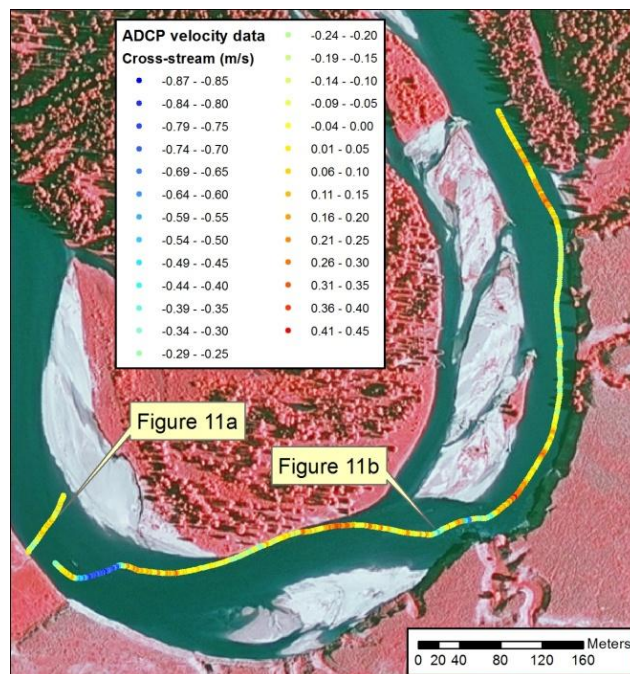


Figure 10. Flow velocity data collected with an acoustic Doppler current profiler (ADCP) along a peculiar meander bend on the Snake River downstream from Pacific Creek. Flow enters from the top of the image, curves to the right around the bend, and exits on the left side of the image. Colored symbols represent the cross-stream component of the depth-averaged velocity vector, with negative values indicating flow toward the right (inner) bank.

summaries of the data, and export the results to a GIS for visualizing the flow data in a spatial context. Figure 11 below illustrates the results of this analysis for a cross-section and longitudinal profile from the same meander bend examined above. This map depicts the depth-averaged cross-stream component of the velocity vector and thus highlights secondary currents associated with point bars. In this representation, negative cross-stream velocities indicate flow toward the right bank (facing downstream). At the upper end of this profile, flow is directed toward the left bank by the bar on the right side of the channel, but a strong current toward the right bank occurs where the terrace on the left bank protrudes into the channel. Water is then deflected back toward the left along the vegetated bank in the middle of the bend and then strongly to the right where the gravel bar on the right side of the channel caused the main talweg to shift toward the outer (left) bank. This complex pattern is associated with the unusual depositional feature on the outer bank near the bend apex. Normally, one would expect sediment deposition to occur on the inner bank, but in this case, the protrusion of the terrace into the channel creates a wake of lower velocity that induces deposition along the left side of the channel. This

example demonstrates the kind of geomorphic insight we hope to gain by collecting additional ADCP data during our upcoming 2011 field campaign.

The code we have developed also allowed us to gain a different perspective on the hydraulic patterns represented in map view in Figure 10. The plots below show the vertical structure of the flow field for a cross-section located downstream of the bend apex and a longitudinal profile through the upper portion of the meander. For the cross-section in Figure 11a, the velocity magnitude and streamwise component were greatest to the left of the channel centerline (i.e., closer to the outer bank). The cross-stream velocity in this region was relatively high and directed toward the outer bank throughout the water column. On the right (inner) half of the channel, cross-stream flow was stronger and directed toward the inner (right) bank near the bed but weaker and outward-directed on the far right side of the transect, where the flow was deflected away from the point bar. These observations are consistent with geomorphic theory for flow around a bend, with a secondary circulation driven by the interaction between the bed topography and inward-directed pressure gradient and outward-directed centrifugal forces. The longitudinal profile highlights similar patterns, with the red tones at a streamwise distance of 4950 m representing the powerful topographic steering that occurs where the flow encounters the large point bar on the right side of the channel and is directed toward the left (outer) bank.

Our future work will involve further collection and analysis of ADCP data with the objective of advancing our understanding of the manner in which river morphology and hydraulics influence sediment transport and ultimately channel change.

◆ MANAGEMENT IMPLICATIONS

This ongoing study directly contributes to the Park Service's current management priorities and could provide a powerful tool for assessment and monitoring of riverine resources throughout the region. The 2009 Craig Thomas Snake River Headwaters Act designated the river above Jackson Lake as a Wild River and the segment from Jackson Lake Dam to Moose, along with the Pacific Creek and Buffalo Fork tributaries, as Scenic Rivers in recognition of their ecological, aesthetic, and recreational value. This legislation provides these streams with protected status as part of the National Wild and Scenic Rivers System and ensures the free-

flowing condition of these waterways. Along with this designation comes the task of determining how best to preserve this remarkable fluvial system. Accordingly, the Park Service has set out to develop a new river management plan, which will involve documenting these unique natural resources and identifying effective strategies for their protection. Park managers are thus obligated to characterize the form and behavior of the Snake River, along with the associated habitat conditions and recreational opportunities. Our primary objective is to derive such information from remotely sensed data; this continuing project will thus directly inform the Park's river Management plan. Moreover, the techniques developed as part of this investigation could be applied to other streams throughout the Snake River

headwaters, both those that have already been awarded Wild and Scenic status and others that might merit such consideration in the future.

Although remote sensing clearly offers significant potential to facilitate a number of river-related applications, this potential has not been realized in practice, and the capabilities and limitations of a remote sensing-based approach must first be established. By demonstrating the utility of these methods, and also acknowledging their deficiencies, this study of the Snake River could lead to more widespread, effective use of remote sensing in river research and management.

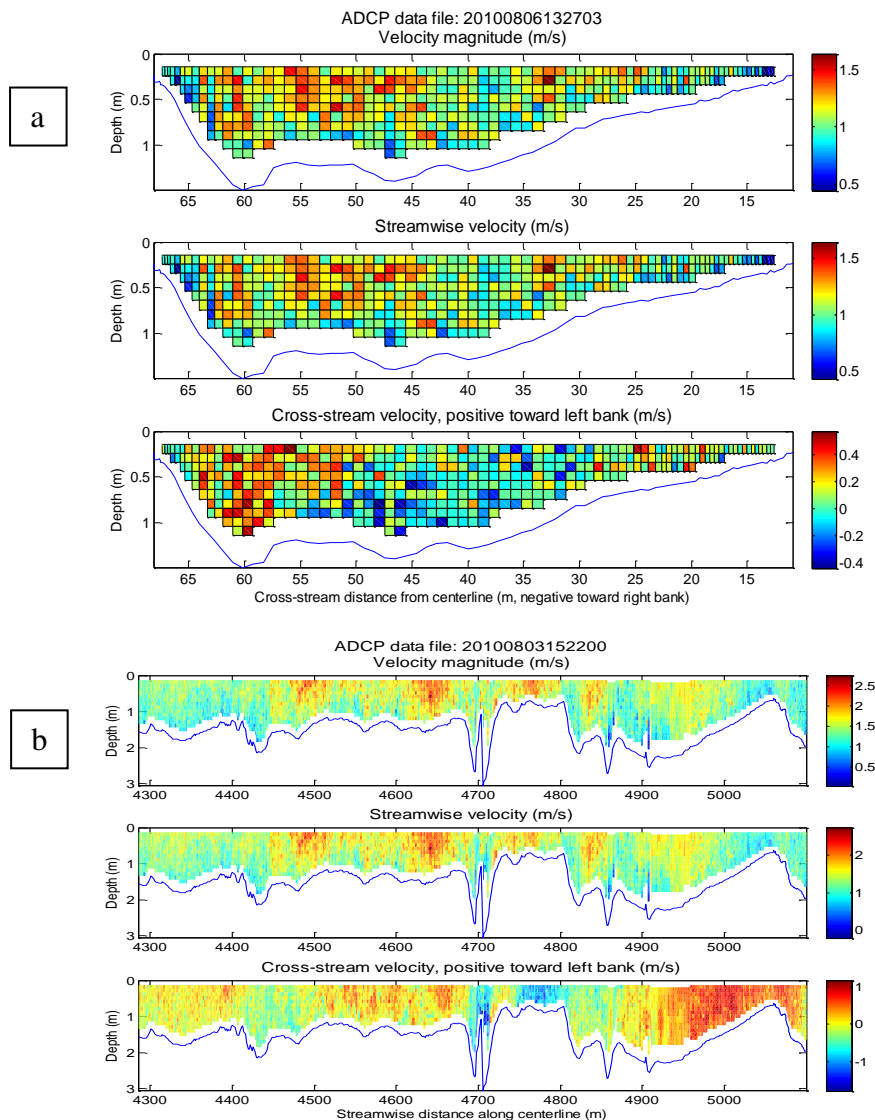


Figure 11. ADCP data collected along the cross-section (a) and longitudinal profile (b) shown in Figure 10. Cross-stream coordinates increase toward the left bank and positive cross-stream velocities indicate flow to the left.

◆ ACKNOWLEDGEMENTS

In addition to support from the UW-NPS Research Station, this project has received key funding from the Office of Naval Research. Field work along the Snake River would not have been possible without the able assistance of Clem Rawlins. Kris Homel provided the 2007 LiDAR data set. Clint Streeter coordinated the Aerocam image acquisition and piloted the aircraft used for data collection. We are grateful to Kathy Mellander and Susan O’Ney of the National Park Service for supporting our study.

◆ LITERATURE CITED

Hofle B, Vetter M, Pfeifer N, Mandlburger G, Stutter J. 2009. Water surface mapping from airborne laser scanning using signal intensity and elevation data. *Earth Surface Processes and Landforms*, 34:1635-1649.

Jones AF, Brewer PA, Johnstone E, Macklin MG. 2007. High-resolution interpretative geomorphological mapping of river valley environments using airborne LiDAR data. *Earth Surface Processes and Landforms*, 32: 1574–1592.

Legleiter CJ, Roberts DA, Marcus WA, Fonstad M. 2004. Passive optical remote sensing of river channel morphology and in-stream habitat: Physical basis and feasibility. *Remote Sensing of Environment*, 93:493–510.

Legleiter CJ, Roberts DA, Lawrence RL. 2009. Spectrally based remote sensing of river bathymetry. *Earth Surface Processes and Landforms*, 34:1039–1059.

Marcus WA, Fonstad MA. 2010. Remote sensing of rivers: the emergence of a subdiscipline in the river sciences. *Earth Surface Processes and Landforms*, 35:1867–1872.

Schmidt JC, Nelson NC. 2007. Hydrology and geomorphology of the Snake River in Grand Teton National Park, WY. Final Report. National Park Service, Washington, DC.

Slatton KC, Carter WE, Shrestha RL, Dietrich WE. 2007. Airborne laser swath mapping: Achieving the resolution and accuracy required for geosurficial research. *Geophysical Research Letters*, 34: doi:10.1029/2007GL031939.